



HAL
open science

Simple Metal-Only 1-Bit Coding Metasurface for RCS Reduction

Thomas Uguen, Raphaël Gillard, Renaud Loison, Jeanne Pagés-Mounic, Philippe Pouliguen

► **To cite this version:**

Thomas Uguen, Raphaël Gillard, Renaud Loison, Jeanne Pagés-Mounic, Philippe Pouliguen. Simple Metal-Only 1-Bit Coding Metasurface for RCS Reduction. 2025 19th European Conference on Antennas and Propagation (EuCAP), Mar 2025, Stockholm, Sweden. pp.1-5, <10.23919/EuCAP63536.2025.10999894>. <hal-05095866>

HAL Id: hal-05095866

<https://hal.science/hal-05095866v1>

Submitted on 4 Jun 2025

HAL is a multi-disciplinary open access archive for the deposit and dissemination of scientific research documents, whether they are published or not. The documents may come from teaching and research institutions in France or abroad, or from public or private research centers.

L'archive ouverte pluridisciplinaire **HAL**, est destinée au dépôt et à la diffusion de documents scientifiques de niveau recherche, publiés ou non, émanant des établissements d'enseignement et de recherche français ou étrangers, des laboratoires publics ou privés.



HAL Authorization

Simple Metal-Only 1-bit Coding Metasurface for RCS Reduction

Thomas Uguen^{*†}, Raphaël Gillard[†], Renaud Loison[†], Jeanne Pagés-Mounic^{*} Philippe Pouliguen[‡]

^{*}CNES, 18 Avenue Edouard Belin, 31400 Toulouse

[†]Univ. Rennes, INSA Rennes, CNRS, IETR-UMR 6164, 35000 Rennes

[‡]DGA-AID, 60 Bd. du général Martial Valin, 75509 Paris

email: Thomas.Uguen@insa-rennes.fr

Abstract—One-bit coding metasurfaces, which combine two basic unit cells with out-of-phase responses, have shown significant potential for achieving diffuse scattering, making them valuable for radar signature control. This paper presents a simple metal-only unit cell to design metasurfaces for radar cross-section reduction. The various steps of designing this unit cell are outlined. The recently introduced Minimum Peak Sidelobes codes in the field of coding metasurfaces, associated with the metal-only unit cell, are being utilized to validate their diffusion capabilities through electromagnetic simulations. The results are compared to those obtained with an analytical approach. To enhance performance and align more closely with the analytical approach, modifications to the unit cell are presented, which involve adding rooftops.

Index Terms—Metal-only, RCS reduction, diffuse scattering, coding metasurface.

I. INTRODUCTION

Among many other possible applications, metasurfaces can be used for radar cross-section (RCS) reduction. A widely used concept in this area is coding metasurfaces [1]. It leverages a limited number of unit cells represented by a binary code. In the simplest implementation, only two coded unit cells are used, labeled as "1" and "0". Thus, the metasurface is encoded using 1-bit representation. The idea behind 1-bit coding metasurface is to reduce the RCS by scattering the incident electromagnetic (EM) wave in all directions. The primary goal when designing such a metasurface is to determine the optimal code to achieve the best diffusion. Several methods are available in the literature, such as the checkerboard configuration [2], [3]. Alternatively, unit cells can be randomly distributed in order to maximize destructive interference, thereby reducing the RCS [4], [5]. Other approaches involves optimization algorithms [6], [7]. Finally, this search for optimal coding is very similar to the one encountered in other scientific domains such as spread spectrum communications [8]. Consequently, codes that have shown good performance there, such as Barker, Golay, or Minimum Peak Sidelobes (MPS) codes can also be applied to design 1-bit coding diffuse scattering metasurfaces [9], [10].

After choosing the coding strategy, several steps are required, including selecting and sizing the two unit cells. Various unit cells such as microstrip patches [1] or metal-only ones [11] are used in the literature. In the context of diffuse

scattering metasurfaces for RCS reduction, microstrip unit cells are widely used. However, due to the presence of a lossy substrate, the infrared (IR) signature may be significant. Moreover, harsh environments, such as space, can present issues for using dielectric materials due to outgassing. In [11], a metal-only metasurface is designed for broadband terahertz RCS reduction and IR invisibility. The metal-only metasurface exhibits extremely low infrared emissivity, unlike metasurfaces designed with microstrip technology.

In this paper, newly introduced MPS codes in [10] are selected to validate their capabilities using EM simulations for the first time. To achieve this, the chosen unit cell is a simple metallic groove to ensure also a low IR signature. It is shown that the use of this unit cell in the metasurface design creates specular reflection issues. Therefore, an evolution of the unit cell is proposed to improve the metasurface performance.

Section II presents the different steps of the metasurface design, starting with the sizing of the unit cell. Once this sizing process is completed, two unit cells are available for the 1-bit coding metasurface implementation. The coding strategy to achieve good diffusion is then presented. Section III provides the EM simulations results for semi-infinite metasurfaces using the metal-only groove unit cell. The simulation environment is detailed beforehand. Then, a technique for reducing the specular reflection specific to this unit cell is introduced and validated.

II. METASURFACE DESIGN

A. Unit cell design

The metal-only unit cell is shown in Figure 1. This unit cell has already been used in [12] for endfire radiation application. It consists of a parallel plate waveguide section with spacing b . The waveguide is shorted at distance h from the aperture. This parameter allows to control the phase-shift encountered by the reflected wave when the cell is illuminated by an x -polarized incident electric field \vec{E}_i . The unit cell is of size $\lambda/2$ in x -direction. Its size is infinite in the y -direction. Indeed, fast validation of MPS codes is desired. Therefore, a 1D scattering scenario is considered here where the metasurface is coded only along the x -axis. The bistatic RCS is then visualized in

the Oxz plane over an elevation angular range from -90° to $+90^\circ$.

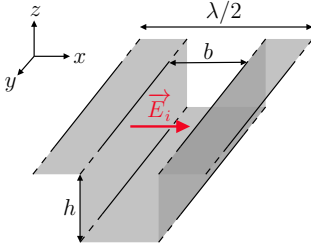


Fig. 1: Geometry of single groove element.

Thus, the unit cell has two degrees of freedom, b and h , representing the width and height, respectively. The width allows for controlling the portion of the incident power transmitted into the groove. It needs to be large enough to ensure that the field is not reflected before it enters the groove. Then, two heights h need to be determined for the design of a 1-bit coding metasurface. These two parameters are determined in the following paragraphs.

The metasurface is designed to operate at 60 GHz. Thus, the size of the unit cell is 2.5 mm in the x -direction. Figure 2 presents the magnitude of the reflection coefficient at the entrance of a matched groove, when b ranges between 1.4 mm and 2 mm, under normal incidence. In this configuration, the groove is matched by replacing the bottom metal plate with a waveguide port. Periodic boundary conditions are used in the Oxz plane. For $b = 2$ mm, $|S_{11}|$ is lower than -18 dB over the 55-65 GHz band. This value is chosen as it provides a good trade-off between efficiency and fabrication complexity. Indeed, a larger b would make the fabrication tricky. For the next step, two different heights h have to be determined to produce expected out-of-phase reflections.

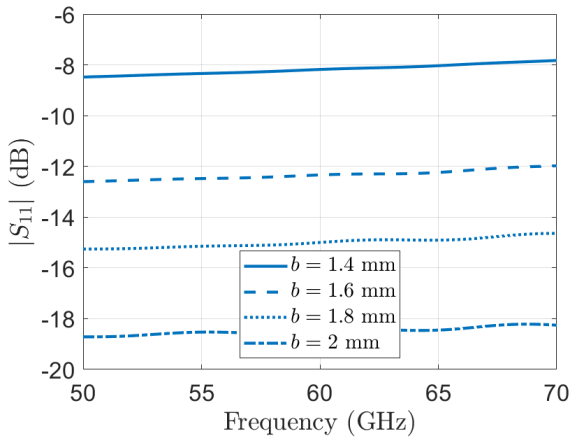


Fig. 2: $|S_{11}|$ parameter for different b in the case of a matched groove, normal incidence illumination.

Figure 3 depicts the reflection coefficient phase at 60 GHz for h varying between 0.2 and 2.6 mm under normal incidence, in the case of the short-circuited groove. These simulations

have been carried out assuming periodicity in the Oxz by simulating a single groove extracted from an infinite periodic array. As discussed before, only two different phase-shifts with a 180° difference are required for 1-bit coding metasurfaces. The two chosen reflection phases here are 30° and -150° . This corresponds to $h_1 = 1.16$ mm and $h_2 = 2.37$ mm respectively. As the metallic groove element has no loss in simulations, the reflection magnitude is 0 dB. In the final metasurface, two consecutive unit cells can be either similar or different, which means the periodicity assumption may be not very realistic in this case. An EM simulation of the complete metasurface, which includes an arrangement of the two different cells, is therefore necessary. The following section covers full-wave simulations of the complete structure.

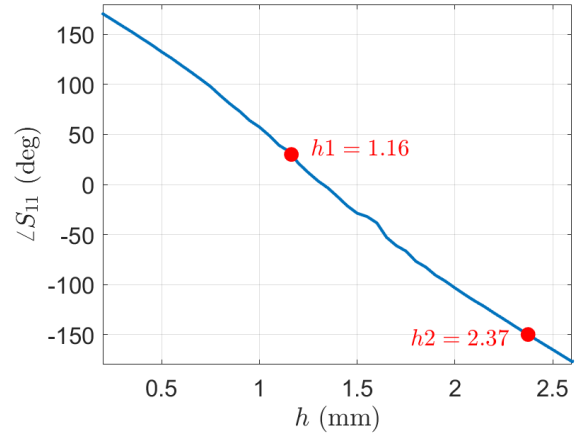


Fig. 3: Reflection phase versus h in the case of the short-circuited groove, $b = 2$ mm, normal incidence illumination.

Figure 4 complements these results by showing the phase difference between the two unit cells across the 50-70 GHz band. It is 180° at 60 GHz, as desired. At higher and lower frequencies, it diverges slightly. Thus, RCS reduction performance is maintained as long as the phase difference remains close to 180° .

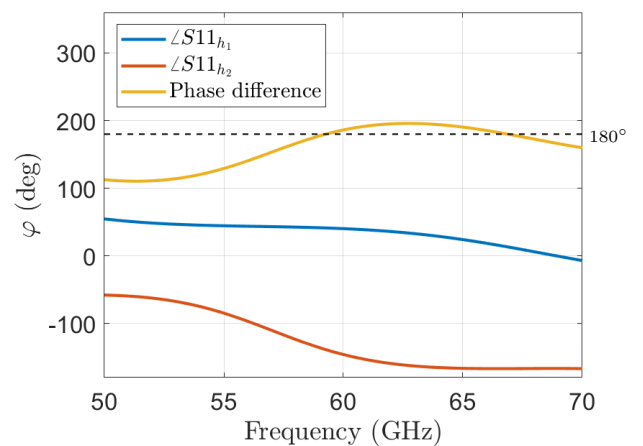


Fig. 4: Phase difference between 0 and 1 unit cells over the 50-70 GHz band.

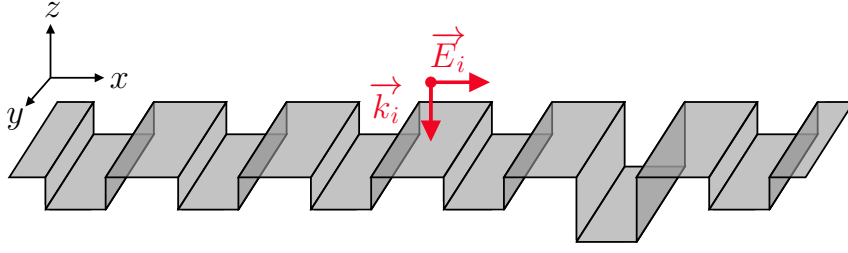


Fig. 5: Metasurface in semi-infinite environment (As an example, the represented code here is 000010 with $N = 6$).

B. Coding strategy

The search for codes that achieve good diffusion is essential before designing the metasurface. Newly introduced MPS codes in [10] are binary codes with optimal or quasi-optimal autocorrelation properties, widely researched across various domains such as spread spectrum [8]. They are also relevant for use in the context of 1-bit coding metasurfaces for RCS reduction as demonstrated in [10]. These codes aim to minimize the peaks of the autocorrelation function, except for the main peak which is equal to N , the size of the binary code. Since deriving MPS codes analytically is challenging, optimization algorithms and exhaustive analyses are used [13], [14]. Many studies have been carried out and a huge quantity of tabulate data is now available for almost any value of N . Indeed, other code families with similar autocorrelation properties, such as Barker or Golay, are limited in terms of size. In [10], a preliminary assessment of the capabilities of MPS codes for RCS reduction by using a simple analytical model for the metasurface scattering is provided. Here, a full demonstration relying on full-wave simulations and considering the implementation of a real unit-cell is proposed.

III. FULL-WAVE SIMULATIONS

A. Simulation environment

The two goals of the following section are to validate, thanks to EM simulations, the implementation of MPS codes and the proposed metal-only unit cell in the context of 1-bit coding metasurfaces for RCS reduction. MPS codes are used here for the design of semi-infinite metasurfaces as shown in Figure 5. For the sake of simplicity, the illustrated example is a metasurface composed of 6 unit cells encoded using the corresponding MPS code [14]. However, the following results are given for a metasurface composed of 32 unit cells. Thus, the corresponding MPS code is 01E5AACC in hexadecimal [14]. The metasurface is illuminated by a plane wave with normal incidence (\vec{k}_i) and polarized along the x -axis. Semi-infinite metasurface means that there are no variations in the code along the y -axis as discussed before in the unit cell design section. To achieve this in a 3D simulation, the boundary conditions must be defined in accordance with the characteristics of the incident wave. The plane wave propagates in z -direction and is polarized along x . Thus, PMC boundaries are assigned to the two side faces parallel to the Oxz plane as shown in

Figure 6. Anisotropic PML are used to absorb the scattering on the surfaces normal to z or x (as can be seen in 6a).

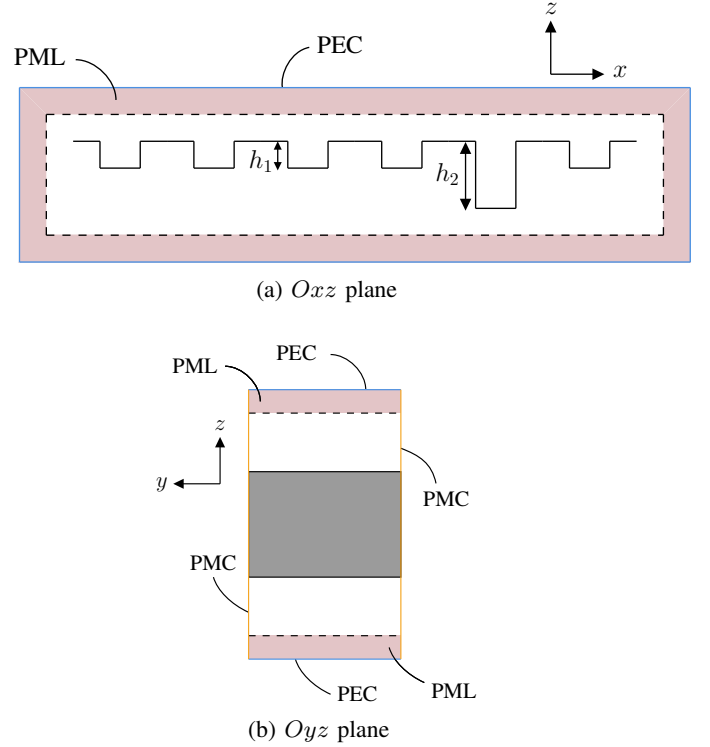


Fig. 6: Cut planes for a semi-infinite environment.

B. Results and discussion

Figure 7 shows the normalized bistatic RCS at 60 GHz. Normalization is performed relatively to a PEC plate of the same size. Effective diffusion of the incident EM wave is achieved, as the field is scattered in all directions. Bistatic RCS reduction ($|\max(\text{RCS}(\theta))_{\text{PEC}} - \max(\text{RCS}(\theta))_{\text{MPS}}|$) is 8.63 dB. The maximum RCS is located in the specular direction. These results are also compared with analytical calculations based on array factor theory [10]. A strong correlation is observed between the analytical calculation and the EM simulation. The reflection minima and maxima align, except in the specular direction. Slight increases are also observed at grazing angles, intuitively linked to the edges of the metasurface that are not taken into account in the analytical model.

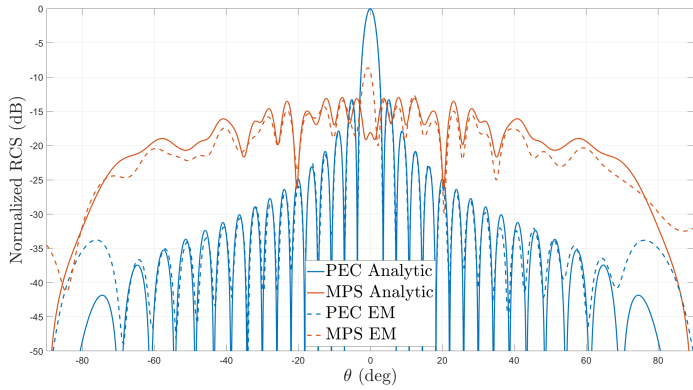


Fig. 7: Normalized bistatic RCS of MPS metasurface, cut plane $\phi = 0^\circ$.

Although the diffusion capability of the MPS code has been demonstrated, its RCS reduction performance is slightly diminished due to specular reflection. The hypothesis is that this significant reflection is related to the upper part of the unit cells arranged in the array. Indeed, two consecutive unit cells form a 0.5 mm wide horizontal metal plate. A method for its suppression is presented in the following section.

C. Specular reflexion cancellation

To reduce the metasurface's specular reflection, rooftops are proposed to be added to the top plates of the semi-infinite metasurface as illustrated in Figure 8.

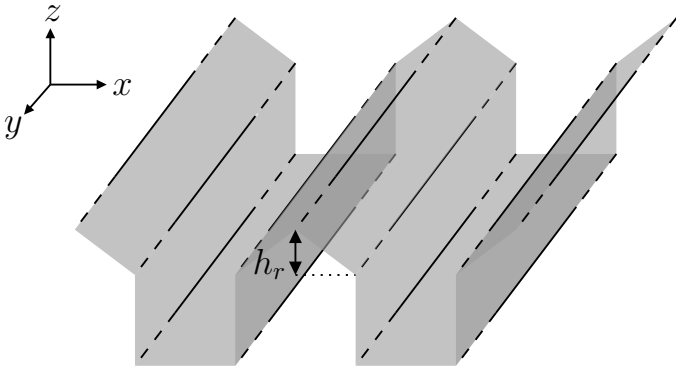


Fig. 8: Two consecutive unit cells with rooftops.

Various heights h_r have been tested through a parametric study. The minimum height is 1 mm to reduce significantly the specular reflection. Figure 9 shows the normalized bistatic RCS of MPS metasurface with 1 mm rooftops at 60 GHz. Bistatic RCS reduction is now 12.97 dB, which gives more than 4 dB improvement compared to the previous configuration. The maximum RCS is no longer in the specular direction but rather around $\theta = -5^\circ$, similar to the analytical calculation. The correlation between the analytical calculation and the EM simulation remains high.

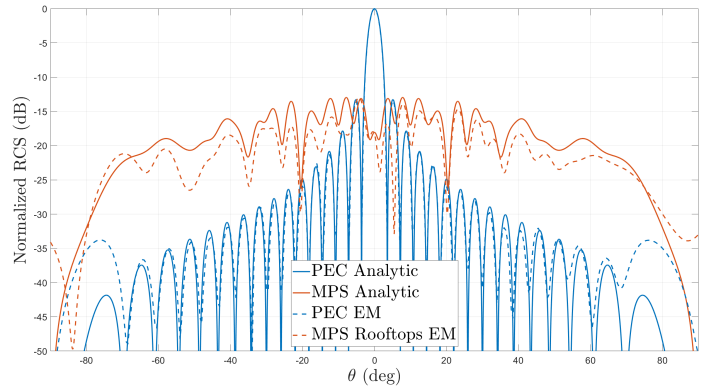


Fig. 9: Normalized bistatic RCS of MPS metasurface with rooftops, cut plane $\phi = 0^\circ$.

D. Bandwidth

To complement the previous results, an RCS reduction study has also been conducted over the 60 ± 10 GHz band. Figure 10 presents the bistatic RCS reduction results over the 60 ± 10 GHz band for semi-infinite metasurfaces, with and without rooftops. The two metasurfaces exhibits good performance across the frequency band. These results are specifically correlated with Figure 4, where the 180° phase difference is generally maintained across this band. Moreover, a significant improvement is observed with the inclusion of rooftops.

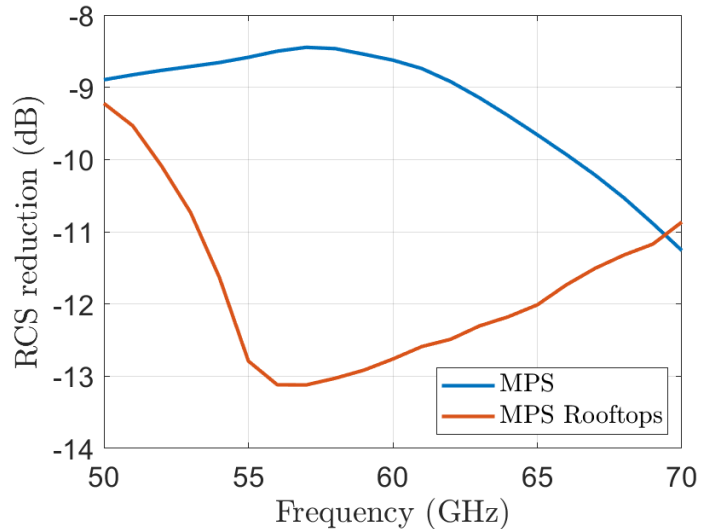


Fig. 10: Bistatic RCS reduction of MPS metasurface over the 60 ± 10 GHz band.

IV. CONCLUSION

This paper introduces a new unit cell in order to design metasurfaces for RCS reduction. Due to its simple geometry, the fabrication process can be straightforward. Additionally, since this unit cell is metal-only, the IR signature should remain low. The new MPS coding for 1-bit diffuse scattering

metasurfaces has also been validated through EM simulations. Finally, the bistatic RCS reduction performance has been improved by modifying the basic unit cell through the addition of rooftops. Future work will focus on the fabrication and measurement of prototypes. Coding in both directions is also planned, involving the development of a new unit cell.

ACKNOWLEDGMENT

This work is funded by the French organizations Centre National des Études Spatiales (CNES) and Agence Innovation Défense (AID).

REFERENCES

- [1] T. J. Cui, M. Q. Qi, X. Wan, J. Zhao, and Q. Cheng, "Coding metamaterials, digital metamaterials and programmable metamaterials," *Light: Science & Applications*, vol. 3, pp. e218–e218, Oct 2014.
- [2] M. Paquay, J.-C. Iriarte, I. Ederra, R. Gonzalo, and P. de Maagt, "Thin amc structure for radar cross-section reduction," *IEEE Transactions on Antennas and Propagation*, vol. 55, no. 12, pp. 3630–3638, 2007.
- [3] W. Chen, C. A. Balanis, and C. R. Birtcher, "Checkerboard ebg surfaces for wideband radar cross section reduction," *IEEE Transactions on Antennas and Propagation*, vol. 63, no. 6, pp. 2636–2645, 2015.
- [4] P. Su, Y. Zhao, S. Jia, W. Shi, and H. Wang, "An ultra-wideband and polarization-independent metasurface for rcs reduction," *Scientific Reports*, vol. 6, p. 20387, Feb 2016.
- [5] Y. Xu, J. Liu, L. Gao, X. Ai, Z. Zhang, and H. Liang, "1-bit coding metasurface for wideband rcs reduction," in *2022 International Applied Computational Electromagnetics Society Symposium (ACES-China)*, pp. 1–3, 2022.
- [6] X. Liu, J. Gao, L. Xu, X. Cao, Y. Zhao, and S. Li, "A coding diffuse metasurface for rcs reduction," *IEEE Antennas and Wireless Propagation Letters*, vol. 16, pp. 724–727, 2017.
- [7] Y. Zhao, X. Cao, J. Gao, Y. Sun, H. Yang, X. Liu, Y. Zhou, T. Han, and W. Chen, "Broadband diffusion metasurface based on a single anisotropic element and optimized by the simulated annealing algorithm," *Scientific Reports*, vol. 6, p. 23896, Apr 2016.
- [8] S. Golomb and G. Gong, *Signal Design for Good Correlation: For Wireless Communication, Cryptography, and Radar*.
- [9] M. Moccia, S. Liu, R. Y. Wu, G. Castaldi, A. Andreone, T. J. Cui, and V. Galdi, "Coding metasurfaces for diffuse scattering: Scaling laws, bounds, and suboptimal design," *Advanced Optical Materials*, vol. 5, no. 19, p. 1700455, 2017.
- [10] T. Uguen, R. Gillard, R. Loison, J. Pagès-Mounic, and P. Pouliguen, "On the use of autocorrelation properties for diffuse reflection by coding metasurfaces," *International Journal of Microwave and Wireless Technologies*, 2024 (Accepted for publication).
- [11] M. Zhang, N. Zhang, P. Dong, L. Yang, B. Wang, R. Wu, and W. Hou, "All-metal coding metasurfaces for broadband terahertz rcs reduction and infrared invisibility," *Photonics*, vol. 10, no. 9, 2023.
- [12] D. Wang, R. Gillard, and R. Loison, "A 60ghz passive repeater array with endfire radiation based on metal groove unit-cells," in *2015 9th European Conference on Antennas and Propagation (EuCAP)*, pp. 1–4, 2015.
- [13] J. Song, P. Babu, and D. P. Palomar, "Optimization methods for designing sequences with low autocorrelation sidelobes," *IEEE Transactions on Signal Processing*, vol. 63, no. 15, pp. 3998–4009, 2015.
- [14] A. N. Leukhin and E. N. Potekhin, "Optimal peak sidelobe level sequences up to length 74," in *2013 European Microwave Conference*, pp. 1807–1810, 2013.